Resonance Raman spectroscopy as an *in-situ* probe for monitoring catalytic events in a Ru-porphyrin mediated amination reaction

Paolo Zardi[a], Emma Gallo[a], Gregory A. Solan[b] and Andrew J. Hudson[b*]

[a] *Dipartimento di Chimica, Università degli Studi di Milano, Via C. Golgi 19, I-20133 Milan, Italy.*

[b] *Department of Chemistry, University of Leicester, Leicester, LE1 7RH, United Kingdom.*

ABSTRACT:

Resonance Raman microspectroscopy has been widely used to study the structure and dynamics of porphyrins and metal complexes containing the porphyrin ligand. Here, we have demonstrated that the same technique can be adapted to examine the mechanism of a homogeneously-catalysed reaction mediated by a transition-metal-porphyrin complex. Previously it has been challenging to study this type of reaction using *in situ* spectroscopic monitoring due to the low stability of the reaction intermediates and elevated-temperature conditions. We have made a straightforward modification to the sample stage on a microscope for time-lapsed Raman microspectroscopy from reaction mixtures in these media. The allylic amination of unsaturated hydrocarbons by aryl azides, which can be catalysed by a ruthenium-porphyrin complex, has been used as an illustrative example of the methodology. The mechanism of this particular reaction has been studied previously using density-functional theory and kinetic approaches. The Raman measurements support the mechanism proposed in the earlier publications by providing the first experimental verification of a precursor reaction complex between the aryl azide and the ruthenium metal ion, and evidence for the formation of a *mono*-imido intermediate complex under conditions of high concentration of the reactant olefin.

*Correspondence to: Dr. Andrew J. Hudson, E-mail: andrew.hudson@leicester.ac.uk.

Introduction

In situ spectroscopic methods are a useful tool to reveal mechanisms of chemical transformations and the identity of reaction intermediates. Of these methods, Raman spectroscopy can be particularly valuable in obtaining structural and electronic information via the determination of frequencies for vibrations of species present in the reaction mixture. Raman approaches have the advantage over infra-red spectroscopy in that the symmetric vibrational modes of molecules can be observed. A significant disadvantage though is that the intensity of Raman-scattered light is usually weak. In resonance Raman spectroscopy, a monochromatic laser is used which is resonant with excited-electronic states of the reactants, intermediates and/or products. This leads to considerable enhancement of Raman cross sections by a factor of 10^3 to 10^5,[1] and has enabled the real-time monitoring of fundamental chemical processes by Raman spectroscopy with nanosecond resolution.[2-5] Continuous-wave lasers have been used in place of pulsed-laser systems to investigate chemical transformations in more complex environments. For example, the prosthetic group in heme proteins is an iron complex, containing the metal in either ferrous or ferric oxidation states, and the ligand protoporphyrin IX. The Raman frequencies of the porphyrin ligand are a sensitive probe of the redox state and the presence of other small molecules bound to the metal centre,[6-8] and can be used to monitor changes in the state of heme proteins *in vivo*.[9-11] We are interested in using the same approach as an *in-situ* probe to monitor the evolving states of a homogeneous catalyst in reactions under working conditions (*e.g.*, elevated temperature and/or pressure). There have been limited attempts to develop such *in situ* techniques suitable to monitor homogeneously-catalysed reactions, however, recently an experimental apparatus was reported for combined UV-Visible absorption, infra red and (non-resonance) Raman spectroscopy using fibre-optic probes but the application of resonance Raman spectroscopy was not explored.[12]

Homogeneous catalysts, based on well-defined transition-metal complexes, are assuming an ever-increasing importance in the production of both commodity and fine chemicals.[13,14] Many of these complexes have absorption bands in the visible region of the electromagnetic spectrum and the frequencies of the Raman transitions will be affected by the redox state of the central-metal ion and the coordinative bonding of reactants, intermediates and/or product molecules to the metal centre. Detailed assignment of resonance Raman spectra in ruthenium metal complexes has been given in the literature for ligands containing pyrrole (porphyrin),[15] pyrazine,[16,17] pyridine,[16,18] and pyrimidine[17] groups, and this earlier work will assist in the analysis of *in situ* experimental spectra obtained during catalytic reactions involving complexes containing the ruthenium metal ion.

An example of particular interest is the allylic amination of cyclohexene by aryl azides using Ru[II](TPP)CO (TPP is the dianion of 5,10,15,20-tetraphenylporphyrin) as the catalyst, which

operates efficiently in refluxing benzene.[19] Such a transformation is representative of a broad class of homogeneously-catalysed reactions (*viz.* metal-catalysed nitrene transfer) that are currently receiving considerable attention as a strategy for preparing desirable nitrogen-containing organic compounds from hydrocarbons.[20-36] Notably the mechanism for this specific amination reaction has been the subject of both a kinetic[37] and a theoretical investigation[38] with the former indicating at least two independent catalytic cycles that depend on the ratio of substrate to aryl azide (see Figure 1). At high cyclohexene concentration the active species was considered to be the *mono*-imido species **B** which is highly reactive and would be immediately trapped by a substrate molecule giving the aminated product **E** whilst re-generating the starting catalyst **A**, Ru(TPP)CO. At low cyclohexene concentration, **B** undergoes a further reaction with the aryl azide giving, via an unstable intermediate **C**, the *bis*-imido complex **D** which is now the active species in allylic amination.[37] Complex **D** is stable and can be isolated from the reaction of **A** with 3,5-*bis*(trifluoromethyl)phenyl azide; however, the isolation of *bis*-imido complexes from aryl azides bearing other electron-withdrawing groups was less successful, and the formation of *bis*-imido complexes from aryl azides bearing electron-donating groups has never been observed.[37] In the presence of these other aryl azides, the catalytic cycle was assumed to be restricted to the example involving the *mono*-imido intermediate **B** due the poor stability of imido derivatives. Direct experimental observation of the *mono*-imido complex **B** has not been made before. Further support for the proposed mechanism has been obtained using density-functional theory[38], while isolable complexes of the type **A** and **D** have been structurally characterised.[19,39]

In this article, we will explore the potential of resonance Raman spectroscopy as a tool to investigate the proposed mechanistic steps for the homogeneously-catalysed reaction shown in Figure 1 at different cyclohexene concentrations. It is envisaged that monitoring the time-dependent shifts in the vibrational modes of the porphyrin skeleton present in the various ruthenium-porphyrin complexes will shed further light on the identity for the intermediate states of the catalyst. Furthermore, we report for the first time a compact piece of apparatus that has been developed for a high temperature application that can be easily transferred to and from a glove box.

Experimental Methods

Amination of an unsaturated hydrocarbon by an aryl azide was catalysed by the ruthenium complex **A**, Ru^{II}(TPP)CO. The reaction was studied using low and high concentrations of the olefin. The solvents, benzene and cyclohexene, used in these experiments were distilled over sodium and stored under nitrogen. Compound **A** was synthesised as described elsewhere.[40]

Low concentration of olefin. 1.85 mg (2.5×10^{-3} mmol) of **A** was dissolved in a mixture of benzene (10 ml) and cyclohexene (114 μL, 1.1 mmol). 3,5-*bis*(Trifluoromethyl)phenyl azide (58 mg, 2.3×10^{-1} mmol) was added under a nitrogen atmosphere, at room temperature, in a glove box.

High concentration of olefin. 1.85 mg (2.5×10^{-3} mmol) of **A** was dissolved in pure cyclohexene (10 ml). 3,5-*bis*(Trifluoromethyl)phenyl azide (13 mg, 5.0×10^{-2} mmol) was added under a nitrogen atmosphere, at room temperature, in a glove box.

It should be noted that in the first experiment a higher azide concentration was used to favour the formation of imido species.

Reaction chamber. For both experiments, 0.5 ml of the reaction mixture was transferred to a custom-designed aluminium chamber, which was closed, under a nitrogen atmosphere in a glove box. The reaction chamber provided an air-tight seal for the reaction mixtures, and enabled homogeneous-catalysed reactions in solvents such as benzene to be monitored at elevated temperature using Raman microspectroscopy. The compact design has not been reported previously. The chamber could be separated into two main parts (**1** and **2**; see Figure 2 **I**). The first part comprised a well (**1**) with an internal volume of approximately 1 ml into which one of the reaction mixtures was placed. A thread on the exterior-cylindrical surface (**3**) enabled the well to be closed, under a nitrogen atmosphere in a glove box, by attaching a collar (**2**) with an internal thread (**4**). A viton o-ring (**5**) was located in a groove machined around the perimeter of the well, and a cover glass (#1.5, 12 mm-diameter; **6**) was placed above the o-ring. When the well was tightened onto the collar (Figure 2 **II**), a seal was obtained between the well and the cover glass. The chamber was inverted to place the reaction mixture in contact with the cover glass (Figure 2 **III**), and remained sealed in this orientation on heating to 70 °C.

Raman microspectroscopy. Raman spectra were recorded from mixtures inside the air-tight chamber on a homebuilt-inverted microscope; described previously.[11] The sample stage consisted of an aluminium plate with a kapton-insulated flexible heater bonded onto the lower surface; the temperature of the aluminium plate was monitored by a PT100 resistance-temperature device and regulated at 70 °C. The sample stage was isolated from the body of the microscope by a 1 cm-thick delrin plate. The sample chamber was placed onto the stage such that the cover glass was aligned with a circular opening in both the aluminium and delrin plates.

An oil-immersion, infinity-corrected, objective lens (1.25 NA) on the microscope was brought into contact with the exterior surface of the cover glass (see Figure 2 **III**) through the opening in the sample stage. The back aperture of the objective lens was overfilled with the 405 nm-beam (Qioptiq, iFLEX; output linewidth reduced by an etalon to 1 cm^{-1}; approximately 1 mW) of a collimated continuous-wave laser. Dichroic mirrors were used to couple the laser light into the imaging optical path and separate the Raman-scattered wavelengths collected by the objective lens from the laser wavelength. Spatial filtering of the Raman scattered light was accomplished by focusing, using a 160 mm achromatic lens, onto a 150 μm pinhole in the confocal image plane. The spatially-filtered light was re-collimated with a second achromatic lens of 160 mm, and then focussed by a 50 mm achromatic lens onto the 100 μm-width entrance slits of a spectrograph with a 0.500 m imaging triple grating monochromator (Acton Research Corporation, Spectra Pro 2500i; 1800 lines/mm grating; 500 nm blaze wavelength). The detector was a -80 °C cooled, back-illuminated, charge-coupled device (Princeton Instruments, Pixis 100B). Spectral data points were measured in increments of 0.018 nm. The optical resolution of the spectroscopic system was 2 cm^{-1}, and the precision for a wavenumber measurement was 0.5 cm^{-1}. The signal-to-noise ratio at the peak position of the ν_4 band of the Ru-porphyrin complex was typically around 40.

Reference solutions. Aniline-coordinated ruthenium complex. Compound **A** (5.0 mg, 6.7×10^{-3} mmol) was suspended in benzene (5 ml) under a nitrogen atmosphere, at room temperature, in a glove box, and an excess of 3,5-*bis*(trifluoromethyl)aniline (**F**; 4.2 μl, 2.7×10^{-2} mmol) was added. The mixture was stirred until it became a red solution. Compound **F** was synthesised using a previously reported procedure.[41]

Allylic amine-coordinated ruthenium complex. The allylic amine product **E**, C_6H_9NHAr (Ar is 3,5-*bis*(trifluoromethyl)phenyl), was synthesised using a literature procedure[37] and a solution of **E** (7.7 mg, 2.5×10^{-2} mmol) was prepared in benzene (5 ml). Compound **A** (3.7 mg, 5.0×10^{-2} mmol) was added to the solution.

Mixture of azide reagent and ruthenium-porphyrin catalyst. Compound **A** (5.0 mg, 6.7×10^{-3} mmol) was suspended in benzene (2 ml) under a nitrogen atmosphere, at room temperature, in a glove box, and an excess of 3,5-*bis*(trifluoromethyl)phenyl azide (12.6 mg, 4.9×10^{-2} mmol) was added. A slight colour change from orange/red to red/brown was observed.

Further reference spectra were recorded for the stable complexes **A**, Ru^{II}(TPP)CO, and **D**, Ru^{VI}(TPP)(NAr)$_2$ (synthesis described elsewhere[19]), and the pure allylic amine **E**. All measurements were made in benzene solutions, at an approximate concentration of 1 mM.

5

Results

Resonance Raman spectroscopy of ruthenium complexes

Raman spectra, between 450 and 1750 cm^{-1}, of ruthenium complexes with 5,10,15,20-tetraphenyl porphyrin (TPP) were obtained using a laser-excitation wavelength of 405 nm. This wavelength is resonant with the Soret absorption band of the ligand. For example, the absorption maximum for the starting catalyst **A**, Ru^{II}(TPP)CO, is 418 nm. The resonance Raman spectra for pure samples of **A** and the intermediate *bis*-imido complex **D**, Ru^{VI}(TPP)(NAr)$_2$, are illustrated in Figure 3.

The spectra for both ruthenium complexes in Figure 3 contain two strong vibrational bands derived from the symmetric ring modes of the porphyrin ligand, ν_4 and ν_2. The assignment of the spectra in Figure 3 is consistent with that reported by Spiro and co-workers.[15] The ν_4 band corresponds to the pyrrole half-ring symmetric stretching vibration and is strongly influenced by the extent of π-backbonding from the metal d orbitals to the porphyrin π^* orbital, where an increase in backbonding decreases the frequency of the ν_4 band. Consequently, both the electron density on ruthenium and the nature of any bond formed by the metal to additional ligands in axial positions has an effect on the position of the ν_4 band. The centre wavelength of ν_4 for the 5-coordinate complex **A** is 1353 cm^{-1}. A significant shift in the position of ν_4 to 1357 cm^{-1} is observed for complex **D** due to the higher oxidation state of the metal centre. The centre position of the ν_2 band for **A** is 1540 cm^{-1} and this band shifts to 1545 cm^{-1} for **D**. Weak vibrational bands are observed in the spectra for the symmetric ν_3 and the asymmetric ν_{12} and ν_{13} ring modes of the porphyrin ligand. A strong band for the stretching mode between the *meso*-C and phenyl groups is observed at 1227 cm^{-1} for **A** and 1233 cm^{-1} for **D**. Additional weaker bands are observed for the stretching vibration between the β-C and H atoms and the phenyl ring modes in the TPP ligand but a displacement in the position of these bands following a change in the oxidation or coordination state of the ruthenium centre was not observed.

There are two bands observed in the spectra shown in Figure 3, which are not derived from the TPP ligand. The Ru-CO stretching band is observed at 525 cm^{-1} in compound **A**, Ru^{II}(TPP)CO. The ν_{12} in-plane ring deformation mode for the 1,3,5-trisubstituted phenyl ligand, Ar, is observed at 1010 cm^{-1} in compound **D**, Ru^{VI}(TPP)(NAr)$_2$. The ν_{12} mode is Raman inactive for the unsubstituted phenyl group in TPP and benzene solvent.

The ν_2 ring-stretching mode for benzene is observed at 991 cm^{-1}, along with weaker bands at 605 cm^{-1} (ν_{18}, ring deformation), 847 & 1176 cm^{-1} (ν_{11} & ν_{17} C-H bending), and 1584 & 1604 cm^{-1} (ν_{16} ring stretching).

The resonance Raman spectra for **A**, $Ru^{II}(TPP)CO$, in the presence of excess 3,5-*bis*(trifluoromethyl)phenyl azide, ArN_3, is shown in Figure 4. There is evidence in this spectrum for the formation of a complex which would be a precursor for the allylic amination reaction illustrated in Figure 1. Tentatively, it could be suggested that the identity of the complex formed is $Ru^{II}(TPP)(ArN_3)CO$; however, this species has been predicted to be weakly bound.[38] The most significant evidence for the formation of a precursor complex is the shift in the $\nu(Ru-CO)$ stretching band from 525 cm^{-1} in the 5-coordinate complex **A** to 497 cm^{-1} following the occupation of the 6th coordination position, *trans* to the CO ligand, on the ruthenium-metal ion. The frequency of the $\nu(Ru-CO)$ band is affected by back-bonding from the Ru d orbitals to the CO π^* orbital. In this case, the reduction in backbonding on ligand binding decreases the bond order of the Ru-CO (metal-to-ligand) bond (whilst increasing the bond order of the C-O bond), leading to a decrease the frequency of the $\nu(Ru-CO)$ band. The CO ligand has a high affinity for the metal d electrons and the degree of back bonding to the CO π^* orbital is very significant in the complex $Ru^{II}(TPP)CO$. The prediction of weak binding between ArN_3 and the ruthenium-metal ion does not entirely preclude the possibility that ArN_3 could act as an electron-withdrawing ligand in the 6th coordinate position, which is favoured by the presence of CF_3 groups on the aryl moiety; this would cause a significant decrease in the back bonding from Ru to the CO π^* orbital, however, this might be expected to increase the order of the Ru-N bond.

It is reported in the literature that the porphyrin ligand in the complexes, $Ru^{II}(TPP)(X)CO$, could be in competition with the CO ligand for the metal d electrons, however, the CO ligand has a much higher affinity for the d electrons than the porphyrin ligand.[15] Consequently, there is a relatively small variation in the frequency of the ν_4 band in $Ru^{II}(TPP)(X)CO$ complexes as back-bonding to the porphyrin ligand is always weak in the presence of an axial CO ligand; ν_4 has been measured from 1350 to 1358 cm^{-1} for the various Ru^{II} complexes in this work. In addition, the frequency of the ν_4 band in the high oxidation state (Ru^{VI}) complex, **D**, is not that much different to the values found in the low oxidation state (Ru^{II}) complexes. This means that the oxidation state of the metal can have only a small effect on the degree of back-bonding to the porphyrin ligand in the presence of an axial CO ligand; *i.e.* the higher electron density on the Ru^{II} metal is re-directed to the CO ligand in preference to the porphyrin ligand. In the complex formed on addition of ArN_3 to $Ru^{II}(TPP)CO$ (see Figure 4), there is a decrease in back-bonding to the CO π^* orbital (described above) and a similar decrease in back-bonding to the porphyrin π^* orbital might also be expected, which would lead to an increase in the ν_4 frequency. The opposite is observed in the experimental data, and a small decrease in the frequency of the ν_4 band from 1353 to 1350 cm^{-1} was measured. We speculate that the reason for this could be the geometry of the resulting complex. The location of a ligand trans to the CO results in strong

overlap between the π orbitals across a planar configuration of axial bonds which has a very substantial effect on the back bonding to the CO π^* orbital. The ligand in the 6th coordinate axial position cannot have such a direct interaction with the porphyrin ligand which is located in a perpendicular plane. The 6th coordinate ligand removes electron density from the Ru-C bond. Most of this electron density is redistributed to π-bonding to the azide group, but it seems likely that, in this configuration, there is also some additional back-bonding interaction to the porphyrin π^* orbital. This causes a small decrease in the frequency of the ν_4 band.

The absence of the aryl ν_{12} band in the spectrum shown in Figure 4 could be due to the weak interaction between ArN$_3$ and ruthenium. Vibrational bands will not be observed in the measured spectrum unless the Raman cross-section is enhanced, via an electronic resonance with the excitation laser mediated by the porphyrin ligand. The centre position of the ν_2 and $\nu(C_m\text{-Ph})$ bands are 1540 cm^{-1} and 1226 cm^{-1}, respectively; similar to the band positions observed for complex **A**. The Raman spectrum reported in Figure 4 indicates an interaction between ArN$_3$ and Ru(TPP)CO and, even if it is not possible to definitively identify the nature of the obtained complex, the immediate formation of a *bis*-imido stable compound **D** can be excluded (see below).

A non-resonance Raman spectrum is shown in Figure 5 (black line) for a solution containing the allylic amine **E**, C$_6$H$_9$NHAr (the product in the scheme shown in Figure 1). All the bands observed in the spectrum correspond to vibrational modes of the benzene solvent. Addition of **E** to **A**, Ru(TPP)CO (in equimolar equivalents), results in the appearance of a resonance Raman spectrum, in which the bands are observed again for the aforementioned porphyrin ligand modes (ν_4 1358 cm^{-1}, ν_2 1545 cm^{-1} and $\nu(C_m\text{-Ph})$ 1231 cm^{-1}) together with the Ru-CO stretching mode and the aryl ν_{12} mode. The appearance of the aryl ν_{12} band suggests that **E** is bound to the 6th coordination position on the ruthenium metal centre to give Ru^{II}(TPP)(**E**)CO in the solution. The resulting complex has a strong fluorescence, with an emission peak maximum >440 nm. The spectra shown in Figure 5 demonstrate clearly that the aryl ν_{12} band is enhanced by an electronic resonance, mediated by the porphyrin ligand, following the binding of the allylic amine **E** to ruthenium; with the Raman scattering cross section correspondingly lower for the free allylic amine in solution. As described above, the CO has a high affinity for the d electrons and backbonding to the porphyrin ligand is weak in complexes containing an axial CO ligand. The effect of binding of **E** to the 6th coordination position appears to have resulted in fact in a slight decrease in backbonding to the porphyrin ligand. The new position of the ν_4 band, at a relatively high wavenumber position of 1358 cm^{-1}, is very similar to that found in the Ru^{VI} complex, **D**, illustrating the point that the larger d electron density in the Ru^{II} complex is mostly redirected to the Ru-CO bond. The secondary amine has exerted little effect on back-bonding to

the CO ligand (or any shift in this band at the much lower frequency of ~520 cm^{-1}, compared to the ν_4 band at ~1350 cm^{-1}, cannot be discerned).

The resonance Raman spectrum obtained following the addition of **F**, ArNH$_2$, to complex **A** is shown at the top of Figure 5. Compound **F** is a by-product of the decomposition of *bis*(trifluoromethyl)phenyl azide, and the presence of Ru^{II}(TPP)(**F**)CO at the conclusion of the catalysed amination reaction is considered likely.[37] The fluorescence of Ru^{II}(TPP)(**F**)CO is considerably lower than Ru^{II}(TPP)(**E**)CO. The ν_4 band for Ru^{II}(TPP)(**F**)CO is centred at 1355 cm^{-1} which is the expected position for ν_4 in a low oxidation-state complex (equivalent to complex **A** in Figure 3) and contrasts with the unusually high value measured for Ru^{II}(TPP)(**E**)CO. The wavenumber positions of the other porphyrin modes for Ru^{II}(TPP)(**F**)CO are similar to those for Ru^{II}(TPP) (**E**)CO: ν_2 1545 cm^{-1} and $\nu(C_m$-Ph) 1230 cm^{-1}. The aryl ν_{12} mode is clearly present in the spectrum of Ru^{II}(TPP)(**F**)CO. The Ru-CO stretching mode has not been resolved clearly though; however, the formation of *bis*-substituted complex in which the CO ligand is replaced by a second aniline molecule is not likely. IR measurements of the purified compound, isolated from benzene solutions, indicate the presence of the C-O stretching band at around 1900 cm^{-1}.[37] In this example, it is proposed that the Ru-CO stretching mode becomes unresolved following the binding of the primary amine **F** to the 6th coordination position on the ruthenium metal ion. Evidence that the ν(Ru-CO) band is not as well resolved following the binding of certain ligands to the 6th coordination position is supported by the data described above for the precursor complex formed between the starting catalyst **A** and ArN$_3$. The resolution of the ν(Ru-CO) band would be more challenging for Ru^{II}(TPP)(**F**)CO, compared with the complex formed between **A** and ArN$_3$, as a result of the increase in fluorescence background in the measured spectrum. The C-O stretching band at around 1900 cm^{-1} is weak in Raman spectra, relative to IR measurements, and it was not resolved above the fluorescence background when the spectral range was extended to higher wavenumbers.

A low power of the 405 nm laser was used in these experiments and there was no evidence of laser photolysis leading to a reduction in the intensity of the Ru-CO band in the resonance Raman spectra.

Ru^{II}(TPP)CO-catalysed amination reaction of unsaturated hydrocarbons by aryl azides

The amination of an unsaturated hydrocarbon by an aryl azide, catalysed by the ruthenium porphyrin complex **A**, Ru^{II}(TPP)CO, was studied under the condition of a low concentration of olefin (1 part cyclohexene to 100 parts benzene). Resonance Raman spectra of the reaction mixture recorded after 0, 8, 20 31, 34.5 and 36 minutes are shown in Figure 6.

The Raman band corresponding to the Ru-CO stretching mode is observed throughout the course of the reaction. The aryl ν_{12} band increases in intensity steadily between 0 and 36 minutes, which implies that either the main product **E** or a by-product, such as **F**, containing the Ar group donated by the aryl azide, remains bonded to the ruthenium catalyst at the conclusion of the reaction. The shift in the position of the ν_4 band during the course of the reaction, at low olefin concentration, is shown in more detail in Figure 7. Although the shift in the centre position of the band, from 1354 cm^{-1} to 1356 cm^{-1}, is relatively small, the peak maximum can be identified precisely in the sequence of spectra as a result of the low noise level leading to signal fluctuations across single pixels only (an error bar of ±1 pixel is shown in Figure 7). No observable shift is observed in the ν_2 band (centre wavenumber, 1543 cm^{-1}). Although there is some evidence of broadening of the $\nu(C_m$-Ph) band, this feature also remains at the same centre position of 1229 cm^{-1}. The fluorescence background increases significantly during the course of the reaction. The final spectrum in Figure 6 should be compared with that reported in Figure 5 for a mixture of the starting catalyst Ru^{II}(TPP)CO, **A**, and compound **E**. It was noted above, unexpectedly, that the position of the ν_4 was similar for **E** and the Ru^{VI} complex **D**.

The catalytic amination reaction was subsequently studied under the condition of a high concentration of olefin (pure cyclohexene; absence of benzene solvent). Resonance Raman spectra of the reaction mixture, recorded at frequent intervals between 0 and 122 minutes, are shown in Figure 8. The 1st and last spectra are also highlighted in the inset across the wavenumber region of the $\nu(Ru$-CO) band; for these highlighted spectra only, the raw data has been background subtracted to remove the broad fluorescence emission underneath the Raman features.

The Raman band corresponding to the Ru-CO stretching mode is observed at a low wavenumber position of 495 cm^{-1} from the onset of the reaction, similar to that shown in Figure 4 following mixing of Ru^{II}(TPP)CO with the aryl azide (see inset in Figure 8). The $\nu(Ru$-CO) band is more difficult to resolve during the course of the reaction, however, by subtracting the fluorescence background, a combination of the low and high wavenumber $\nu(Ru$-CO) bands is observed (see inset in Figure 8), corresponding to a mixture of imido complex, $\nu(Ru$-CO) at 495 cm^{-1}, and Ru^{II} complexes, $\nu(Ru$-CO) ~520 cm^{-1}. Once again, the aryl ν_{12} band increases in intensity during the course of the catalytic reaction, indicating that a ligand containing the 3,5-*bis*(trifluoromethyl)phenyl substituent remains bound to the ruthenium metal centre as the reaction proceeds. The shift in the position of the ν_4 and $\nu(C_m$-Ph) bands is shown in more detail in Figure 9. Once again, the overall shift in peak positions is relatively small but the low noise level leads to signal fluctuations across single pixels only (an error bar of ±1 pixel is shown in Figure 9). The centre position of the ν_4 band shifts from 1354 to 1358 cm^{-1} after approx. 27.5

minutes, and back to 1355 cm^{-1} after 95 - 108 minutes of the reaction; the centre position of the ν(C$_m$-Ph) band shifts from 1226 to 1231 cm^{-1} after 12.5 minutes of the reaction. As in the previous example at low olefin concentration, there is no observable shift seen in the ν_2 band (centre wavenumber is 1545 cm^{-1}) and the fluorescence increases during the course of the reaction at high olefin concentration. The latter result is consistent with the eventual coordination of the allylic amine product **E** to the ruthenium metal centre. At low olefin concentration, there were no further changes in the Raman spectrum after 36 minutes; in contrast, at high concentration of olefin, there were significant changes in the Raman spectrum for up to 122 minutes.

Discussion

Low concentration of olefin.

The mechanism of the ruthenium-catalysed amination reaction proposed,[37] and illustrated in Figure 1, suggests that a *bis*-imido complex **D**, Ru^{VI}(TPP)(NAr)$_2$, is formed as an intermediate at low olefin concentration. The persistence of the Ru-CO stretching band in the Raman spectra indicates that part of the catalyst is not converted to the *bis*-imido complex at any stage of the reaction; the most likely explanation is that the reaction is taking place via both cycles shown in Figure 1. The increase in the fluorescence background is consistent with the coordination of the allylic amine product **E**, C$_6$H$_9$NHAr, to the 6th position on the ruthenium metal centre, in either unreacted or recovered complex **A**, to give Ru^{II}(TPP)CO**E**.

The exact identification of intermediates or products from the positions of various bands (ν_2, ν_4 and ν (C$_m$-Ph)) in the Raman spectra cannot be made. These bands are relatively broad in the measured spectra and, in the course of the reaction, must contain unresolved contributions from different species. As noted above, it is suspected that the reaction could be taking place via both cycles shown in Figure 1. The shift in the position of the pyrrole half-ring symmetric-stretching vibraton, ν_4, observed during the catalysed reaction is similar to that observed either following an oxidation state change of the metal centre (Ru^{II} → Ru^{VI}) or the binding of the allylic amine **E** to the 6th coordination position in the ruthenium complex (Ru^{II}(TPP)CO + E → Ru^{II}(TPP)CO**E**). The strong fluorescence is further evidence for the binding of the target product **E** to the ruthenium metal centre. Since the by-product **F** proposed in reference 37 has been shown to give a complex with low fluorescence intensity on binding to the vacant coordination site in **A**, it seems likely that the target product **E** is dominant in the final mixture. The final spectrum in Figure 7 shows a ν(Ru-CO) band (following fluorescence background subtraction) which could suggest a mixture of Ru^{II}(TPP)CO**E** and the starting catalyst **A**.

High concentration of olefin.

The previously proposed mechanism for the ruthenium-catalysed amination reaction,[37] and illustrated in Figure 1, suggested that a *mono*-imido complex **B**, $Ru^{IV}(TPP)(NAr)CO$, is formed as an intermediate at high olefin concentration. This is supported by the appearance of the ν(Ru-CO) band at a low wavenumber position as a result of the binding of the imido group to the 6th coordination position on ruthenium in a *trans* geometry with the CO ligand; a similar low wavenumber for the ν(Ru-CO) band was observed for the supposed azide complex. A combination of the low and high wavenumber ν(Ru-CO) bands is observed during the course of the reaction, and it is likely that a mixture of imido complex, at low ν(Ru-CO), and Ru^{II} complexes, at high ν(Ru-CO), exist at the conclusion of the reaction. This result supports the proposal of complex **B** as a reaction intermediate following the theoretical study published earlier.[38] This is further substantiated by shifts in the ν_4 and $\nu(C_m$-Ph) bands to higher wavenumbers during the initial 27.5 minutes of the reaction consistent with an intermediate, such as the *mono*-imido complex **B** (Ru^{IV}), with a high oxidation state being dominant in the reaction mixture. The subsequent decrease in the wavenumber position for the ν_4 band after 95 - 108 minutes of the reaction supports the proposed mechanism that reduction of complex **B** (Ru^{IV}) takes place to give a final resting state for the catalyst as a Ru^{II} complex.

The increase in the fluorescence background during the course of the reaction at high olefin concentration is consistent with the binding of allylic amine product **E** to the ruthenium complex to give $Ru^{II}(TPP)CO$**E**. There are two notable differences though in comparing the results obtained at high and low concentrations of the olefin. In the previous example at low olefin concentration, (i) the ν(Ru-CO) band was resolved clearly at the high wavenumber position, and (ii) the position of the ν_4 band did not shift back to a lower wavenumber at the conclusion of the reaction. In the present example, at high olefin concentration, the initial increase followed by a decrease in the wavenumber position of the ν_4 band is as might have been expected for the proposed reaction mechanism shown in Figure 1; *i.e.* the ν_4 band shifts to a higher wavenumber position as a consequence of the formation of complex **B** (Ru^{IV}) but then returns to a lower wavenumber position as a consequence of the recovery of the Ru^{II} oxidation level in the resting state of the catalyst.

Conclusion

The resonance Raman spectra recorded during the course of the chemical reaction support the mechanistic proposal for the formation of (i) a precursor complex between the starting catalyst, Ru(TPP)CO, and the aryl azide and (ii) a *mono*-imido intermediate, $Ru^{IV}(TPP)(NAr)CO$, at high concentrations of olefin. Both of these complexes were proposed earlier on the basis of theoretical studies. The new experimental data also suggests that a *mono*-imido intermediate could exist transiently only for low concentrations of olefin, where the formation of a *bis*-imido $Ru^{VI}(TPP)(NAr)_2$ catalytic active species was already proposed. The resonance Raman spectra have provided a clear indication of the resting state of the metal complex catalyst in solution, with the allylic amine product binding to the 6th coordination position on the metal centre to produce a fluorescent complex.

The same methodology that was used in this work to study the amination of unsaturated hydrocarbons by aryl azides could be used to investigate other homogeneous reactions catalysed by transition-metal complexes. Conditions for resonance Raman spectroscopy would need to be achieved by appropriate selection of the excitation wavelength. In the present example, both redox changes and ligand binding/substitution steps involving the ruthenium-porphyrin catalyst could be determined during the course of reactions by the use of a 405 nm laser, which is resonant with the Soret absorption band of the porphyrin ligand. For another example, a different wavelength will be required which is resonant with any of the absorption features of the catalyst, which could include d-d transitions of the metal, however, a stronger enhancement of Raman bands is likely from resonance with the absorption features for one of the ligand groups. A relatively straightforward sample chamber has been constructed that can be sealed, containing the reaction mixtures, inside a glove box, and transferred to a heated microscope stage in order to monitor the ensuing reaction *in situ* by resonance Raman spectroscopy. In the present example, a temperature of 70 °C was used to achieving refluxing conditions in benzene; any other temperature up to this value could be used but this was the highest accessible temperature for which stable focussing of the confocal Raman microscope could be maintained.

Figure captions

Figure 1: Proposed mechanism for the $Ru^{II}(TPP)CO$-catalysed amination reaction of cyclohexene by aryl azides; adapted from reference 37.

Figure 2: Custom-designed sealed reaction chamber. **I.** The chamber comprises a well (**1**) with an internal volume of approx. 1 ml and a cap (**2**). A male-thread on the well (**3**) and a female-thread on the collar (**4**) enables the contents to be sealed, under a nitrogen atmosphere in a glove box, by tightening to bring a viton o-ring (**5**) in contact with a #1.5-sized cover glass (**6**). **II.** The chamber is inverted placing the reaction mixture in contact with the cover glass. **III.** Raman microspectroscopy can be performed by positioning the objective lens of an inverted microscope in contact with the cover-glass window.

Figure 3: Resonance Raman spectra of ruthenium complexes. Red – $Ru^{II}(TPP)CO$ (**A**). Green – $Ru^{VI}(TPP)(NAr)_2$ (**D**).

Figure 4: Resonance Raman spectra of $Ru^{II}(TPP)CO$ (**A**) in the presence of excess ArN_3.

Figure 5: Black - Non-resonance Raman spectrum of the allyl amine, $ArNH(C_6H_9)$ (**E**). Red - Resonance Raman spectrum recorded from a mixture of $Ru^{II}(TPP)CO$ (**A**) and **E**. Blue - Resonance Raman spectrum recorded from a mixture of **A** and $ArNH_2$ (**F**).

Figure 6: Time-lapse resonance Raman spectra of the catalytic reaction mixture under the conditions of low olefin concentration.

Figure 7: The observed shift in the ν_4 band observed by resonance Raman spectra in the catalysed-amination reaction mixture under the conditions of low olefin concentration.

Figure 8: Time-lapse resonance Raman spectra of the catalytic reaction mixture under the conditions of high olefin concentration. Inset – The $\nu(Ru\text{-}CO)$ band in the first and last spectra (corrected for the fluorescence background).

Figure 9: The observed shift in the $\nu(C_m\text{-}Ph)$ and ν_4 bands observed by resonance Raman spectra in the catalysed-amination reaction mixture under the conditions of high olefin concentration.
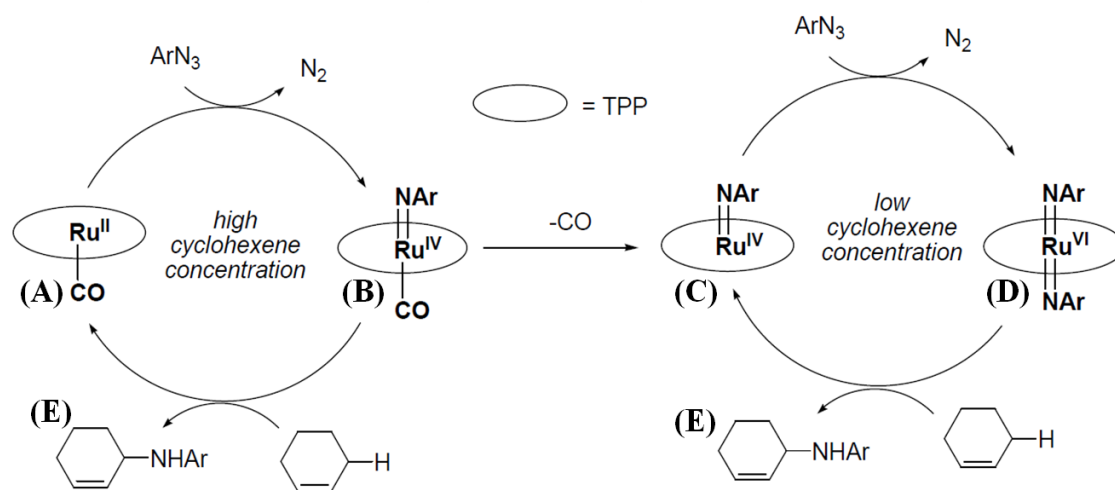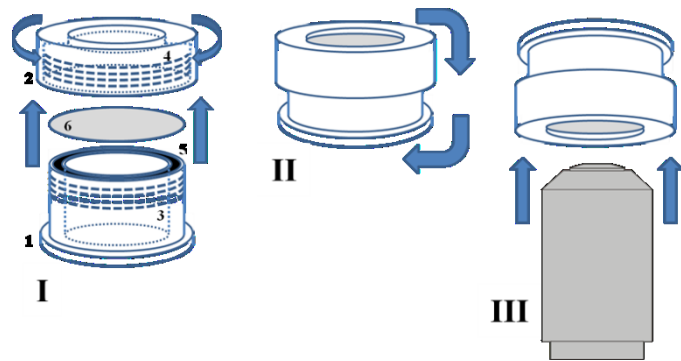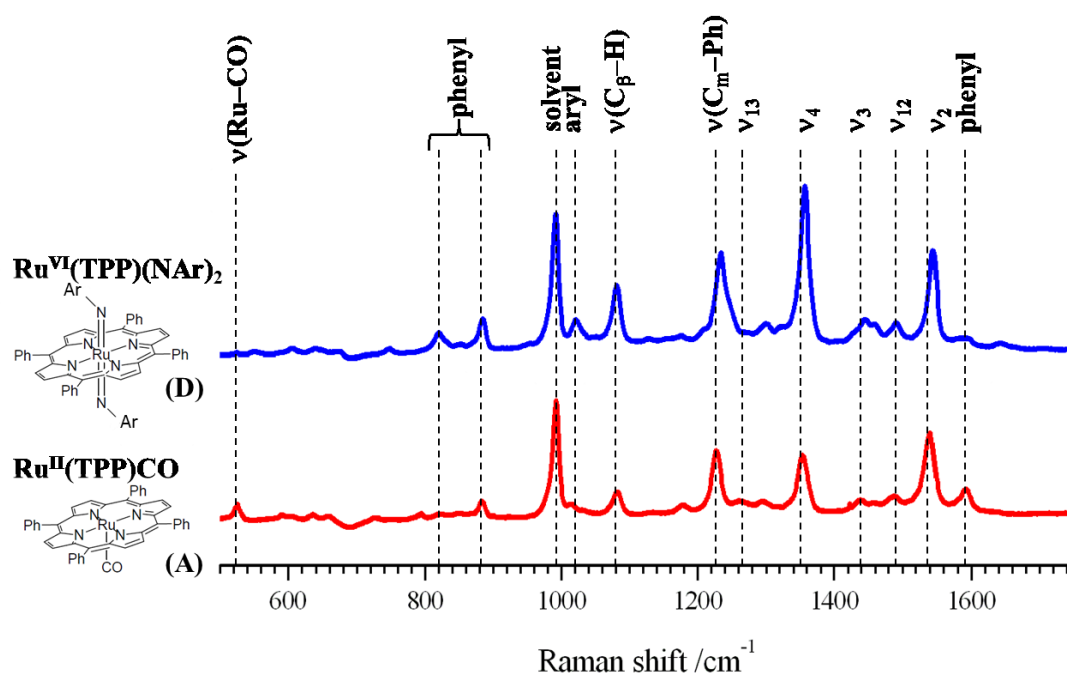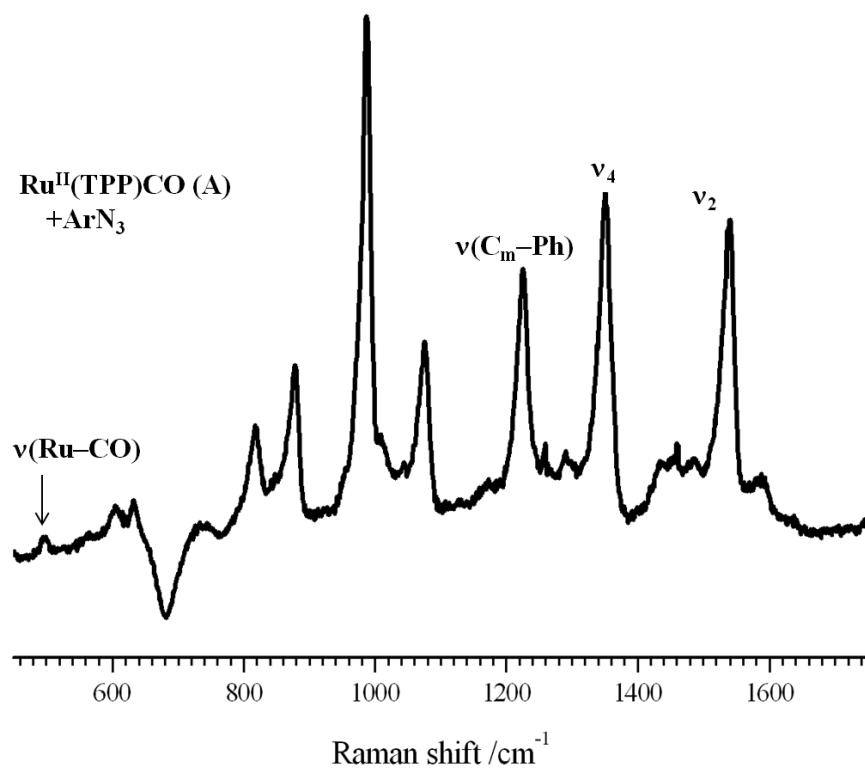
Figure 1

Figure 2

Figure 3

Figure 4
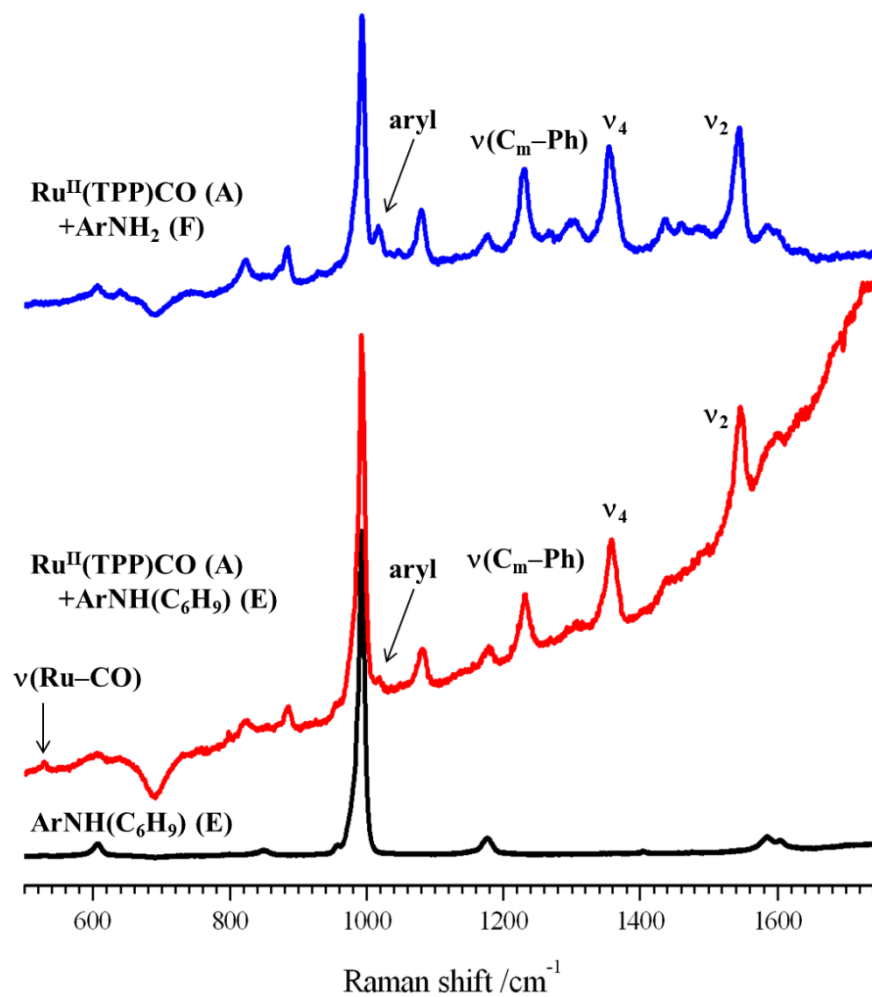
Figure 5
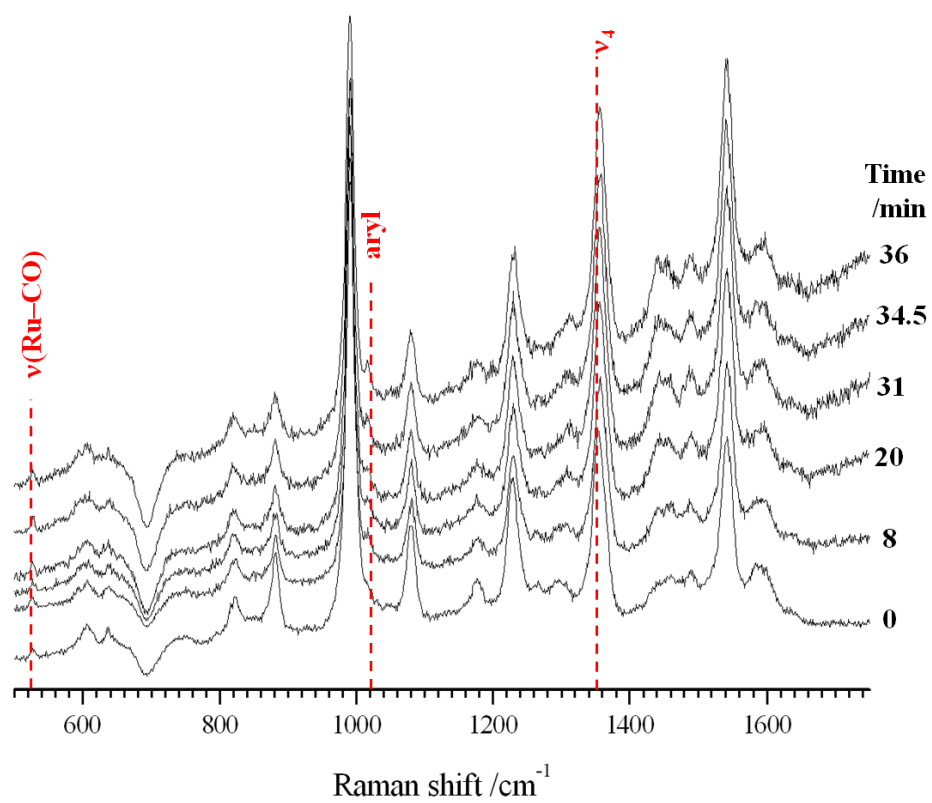
Figure 6

Figure 7

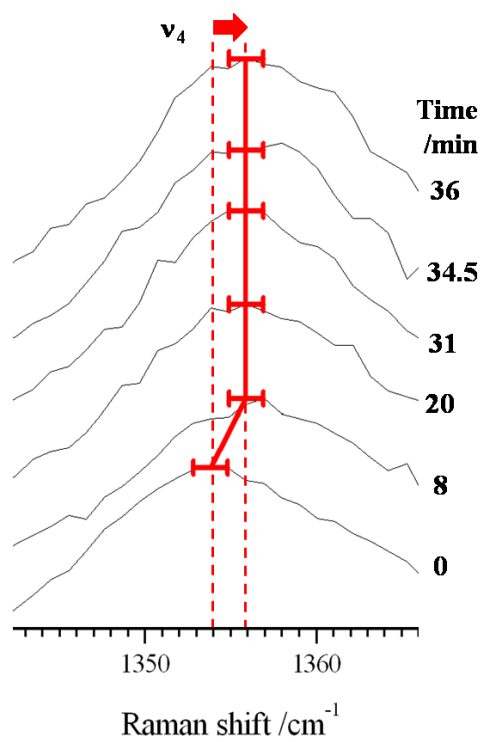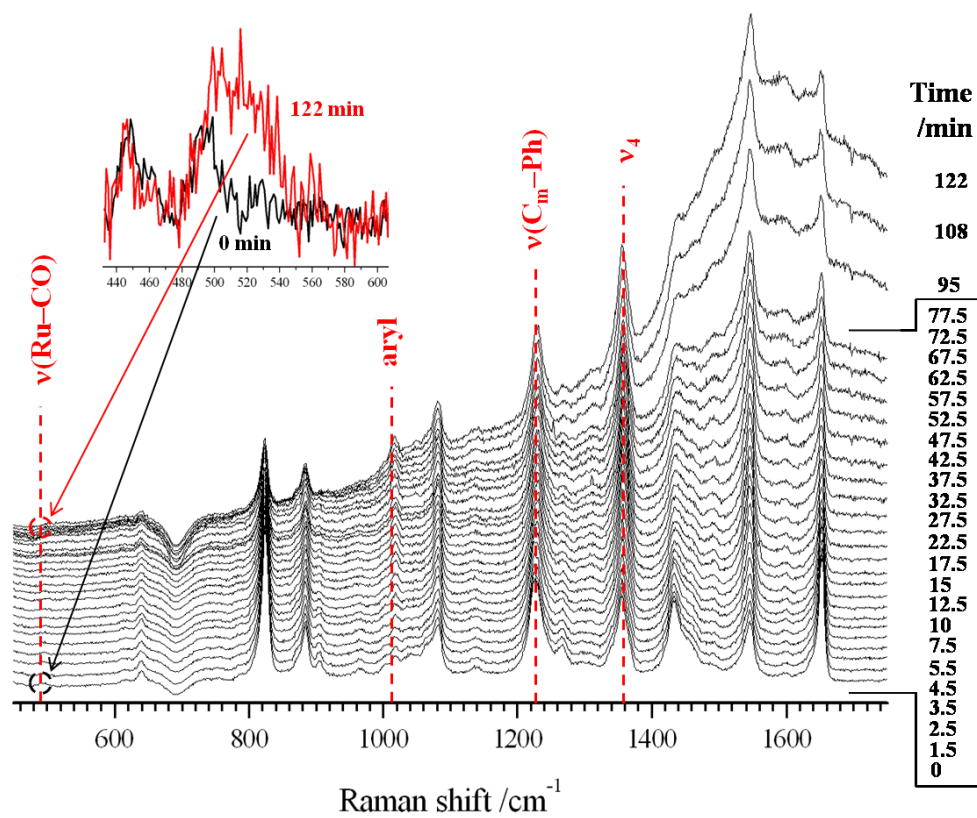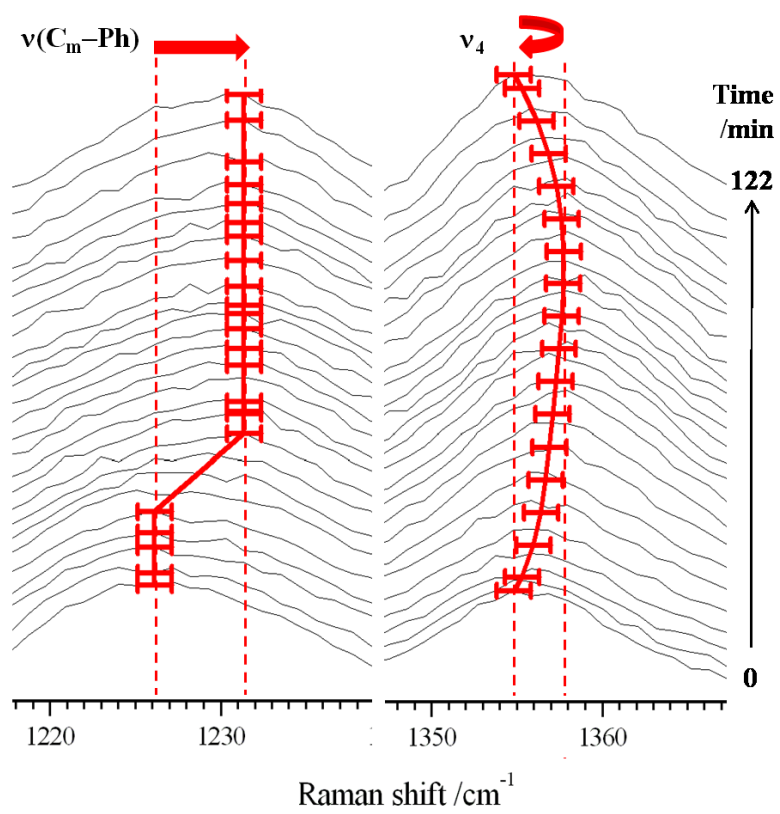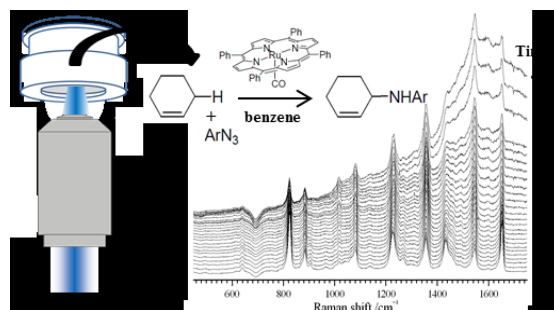**Figure 8**

Figure 9

Table of Contents Graphic

Text: A method to monitor the mechanisms of homogeneously-catalysed reactions under conditions of refluxing solvents using resonance Raman spectroscopy

[1] J. R. Ferraro and K. Nakamoto, Introductory Raman Spectroscopy, Academic Press: New York, **1994**.

[2] P. Pagsberg, R. Wilbrandt, K. B. Hansen and K. V. Weisberg, *Chem. Phys. Letts.*, 1976, **39**, 538-541.

[3] E. Vauthey, D. Phillips and A. W. Parker, *J. Phys. Chem.*, 1992, **96**, 7356-7360.

[4] S. E. J. Bell, *Analyst*, 1996, **121**, R107-R120.

[5] Y. L. Li, K. H. Leung and D. L. Phillips, *J. Phys. Chem. A.* 2001, **105**, 10621-10625.

[6] S. Hu, K. M. Smith and T. G. Spiro *J. Am. Chem. Soc.* 1996, **118**, 12638–12646.

[7] S. Hu, I. K. Morris, J. P. Singh, K. M Smith and T. G. Spiro, *J. Am. Chem. Soc.* 1993, **115**, 12446–12458.

[8] T. G. Spiro and T. C. Strekas, *J. Am. Chem. Soc.* 1974, **96**, 338–345.

[9] K. R. Ward, I. Torres Filho, R. W. Barbee, L. Torres, M. H. Tiba, P. S. Reynolds, R. N. Pittman, R. R. Ivatury and J. Terner, *Crit. Care Med.* 2006, **34**, 792–799.

[10] K. R. Ward, R. W. Barbee, P. S. Reynolds, I. P. Torres Filho, M. H. Tiba, L. Torres, R. N. Pittman and J. Terner, *Anal. Chem.* 2007, **79**, 1514–1518.

[11] A. Almohammedi, S. M. Kapetanaki, B. R. Wood, E. L. Raven, N. M. Storey and A. J. Hudson, *J. R. Soc. Interface* 2015, **12**, 20141339.

[12] K. Grabow and U. Bentrup, *ACS Catalysis* 2014, **4**, 2153-216.

[13] P. W. N. M. Leeuwen, Homogeneous Catalysis: Understanding the Art, Kluwer: Dordrecht, 2004.

[14] S. Bhaduri and D. Mukesh, Homogeneous Catalysis: Mechanisms and Industrial Applications, 2nd Edtn., John Wiley & Sons: New York 2014.

[15] D. Kim, Y. O. Su and T. G. Spiro, *Inorg. Chem.* 1986, **25**, 3993-3997.

[16] G. D. Danzer, J. A. Golus and J. R. Kincaid, *J. Am. Chem. Soc.* 1993, **115**, 8643-8648.

[17] G. D. Danzer and J. R. Kincaid, *J. Phys Chem.* 1990, **94**, 3976-3980.

[18] D. J. Ma'nuel, D. P. Strommen, A. Bhuiyan, M. Sykora and J. R. Kincaid, *J. Raman Spectroscopy* 1997, **28**, 933-938.

[19] S. Fantauzzi, E. Gallo, A. Caselli, F. Ragaini, N. Casati, P. Macchi and S. Cenini, *Chem. Commun.* 2009, 3952-3954.

[20] J. T. Groves and T. Takahashi, *J. Am. Chem. Soc.* 1983, **105**, 2073-2074.

[21] G.-Y. Gao, J. E. Jones, R. Vyas, J. D. Harden and X. P. Zhang, *J. Org. Chem.* 2006, **71**, 6655-6658.

[22] W. Xiao, J. Wei, C.-Y. Zhou and C.-M. Che, *Chem. Commun.* 2013, **49**, 4619-4621.

[23] J. V. Ruppel, J. E. Jones, C. A. Huff, R. M. Kamble, Y. Chen and X. P. Zhang, *Org. Lett.* 2008, **10**, 1995-1998.

[24] Y. Liu and C.-M. Che, *Chem. Eur. J.* 2010, **16**, 10494-10501.

[25] J. P. Mahy, G. Bedi, P. Battioni and D. Mansuy, *New J. Chem.* 1989, **13**, 651-657.

[26] J. P. Mahy, P. Battioni and D. Mansuy, *J. Am. Chem. Soc.* 1986, **108**, 1079-1080.

[27] J.-L. Liang, J.-S. Huang, X.-Q. Yu, N. Zhu and C.-M. Che, *Chem. Eur. J.* 2002, **8**, 1563-1572.

[28] X.-G. Zhou, X.-Q. Yu, J.-S. Huang and C.-M. Che, *Chem. Commun.* 1999, 2377-2378.

[29] X. Q. Yu, J. S. Huang, X. G. Zhou and C. M. Che, *Org. Lett.* 2000, **2**, 2233-2236.

[30] S.-M. Au, W.-H. Fung, M.-C. Cheng, C.-M. Che and S.-M. Peng, *Chem. Commun.* 1997, 1655-1656.

[31] S.-M. Au, J.-S. Huang, W.-Y. Yu, W.-H. Fung and C.-M. Che, *J. Am. Chem. Soc.* 1999, **121**, 9120-9132.

[32] C.-M. Che and W.-Y. Yu, *Pure Appl. Chem.* 1999, **71**, 281-288.

[33] J. P. Mahy, G. Bedi, P. Battioni and D. Mansuy, *J. Chem. Soc., Perkin Trans. 2* 1988, 1517-1524.

[34] J.-P. Simonato, J. Pecaut, J.-C. Marchon and W. R. Scheidt, *Chem. Commun.* 1999, 989-990.

[35] J.-L. Liang, S.-X. Yuan, J.-S. Huang, W.-Y. Yu and C.-M. Che, *Angew. Chem. Int. Ed.* 2002, **41**, 3465-3468.

[36] X. Lin, C.-M. Che and D. L. Phillips, *J. Org. Chem.* 2008, **73**, 529-537.

[37] D. Intrieri, A. Caselli, F. Ragaini, P. Macchi, N. Casati and E. Gallo, *Eur. J. Inorg. Chem.* 2012, 569-580.

[38] G. Manca, E. Gallo, D. Intrieri and C. Mealli, *ACS Catalysis* 2014, **4**, 723-832.

[39] Z. Guo, X. Guan, J.-S. Huang, W.-M. Tsui, Z. Lin and C.-M. Che, *Chem. Eur. J.* 2013, **19**, 11320-11331.

[40] E. Gallo, A. Caselli, F. Ragaini, S. Fantauzzi, N. Masciocchi, A. Sironi and S. Cenini, *Inorg. Chem.* 2005, **44**, 2039-2049.

[41] M. Tanno, S. Sueyoshi and S. Kamiya, *Chem. Pharm. Bull.* 1982, **30**, 3125–3132.